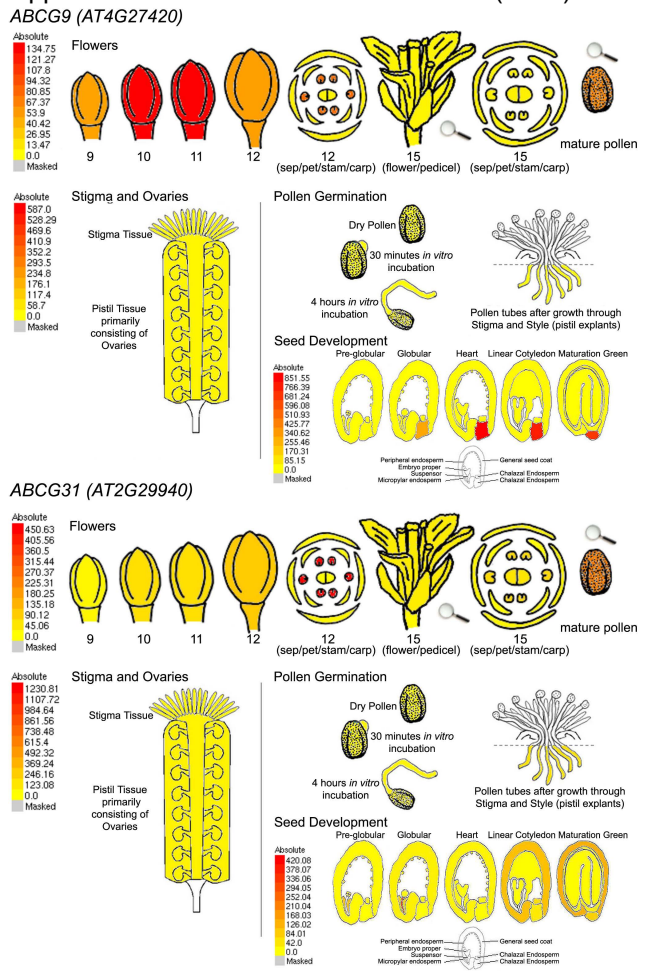

Supplemental Figure 1. Expression patterns of *ABCG9* and *ABCG31* in flowers and developing seeds, according to the BAR Arabidopsis eFP browser.

The expression values of *ABCG9* and *ABCG31* in developing flowers, developing pollen grains, stigmas and ovaries, dry or germinating pollen grains, and developing seeds were obtained from a public microarray database, the BAR Arabidopsis eFP browser (http://bar.utoronto.ca/efp/cgi-bin/efpWeb.cgi).

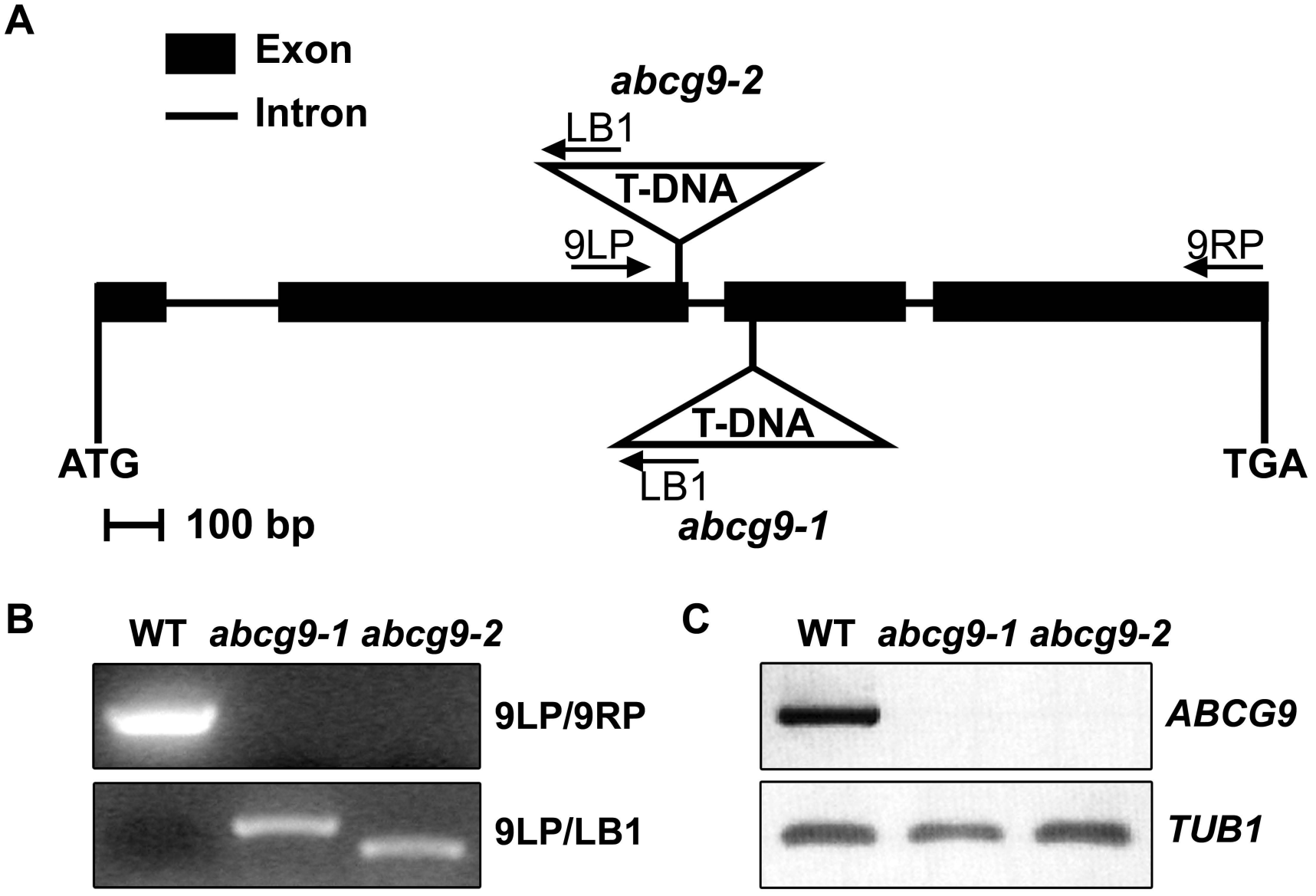

Supplemental Figure 2. Isolation of *abcg9* knockout mutant plants.

(A) Structure of *ABCG9*, with the positions of the T-DNA insertion sites indicated by flags. Exons and introns are denoted by black boxes and lines, respectively. Arrows indicate the positions of primers. (B) Genomic DNA-PCR analysis of *ABCG9*. Total genomic DNA was extracted from the rosette leaves of wild-type, *abcg9-1,* and *abcg9-2* plants. (C) Reverse transcriptase (RT)-PCR analysis of *ABCG9* expression. Total RNA was extracted from the flowers of wild-type, *abcg9-1,* and *abcg9-2* plants. *β-tubulin* (*TUB1*) was used as an internal control.

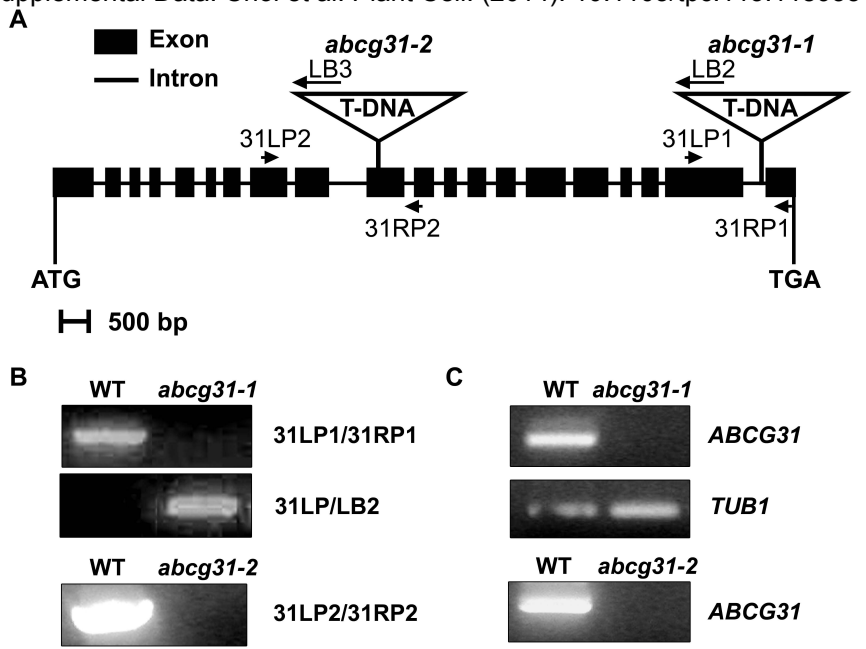

Supplemental Figure 3. Isolation of *abcg31* knockout mutant plants.

(A) Structure of *ABCG31*, with the positions of the T-DNA insertion sites indicated by flags. Exons and introns are denoted by black boxes and lines, respectively. Arrows indicate the positions of primers. (B) Genomic DNA-PCR analysis of *ABCG31*. Total genomic DNA was extracted from the rosette leaves of wild-type, *abcg31-1,* and *abcg31-2* plants. (C) RT-PCR analysis of *ABCG31* expression. Total RNA was extracted from the flowers of wild-type, *abcg31-1,* and *abcg31-2* plants. *β-tubulin* (*TUB1*) and *ubiquitin* (*UBQ1*) were used as internal controls for *abcg31-1* and *abcg31-2*, respectively.

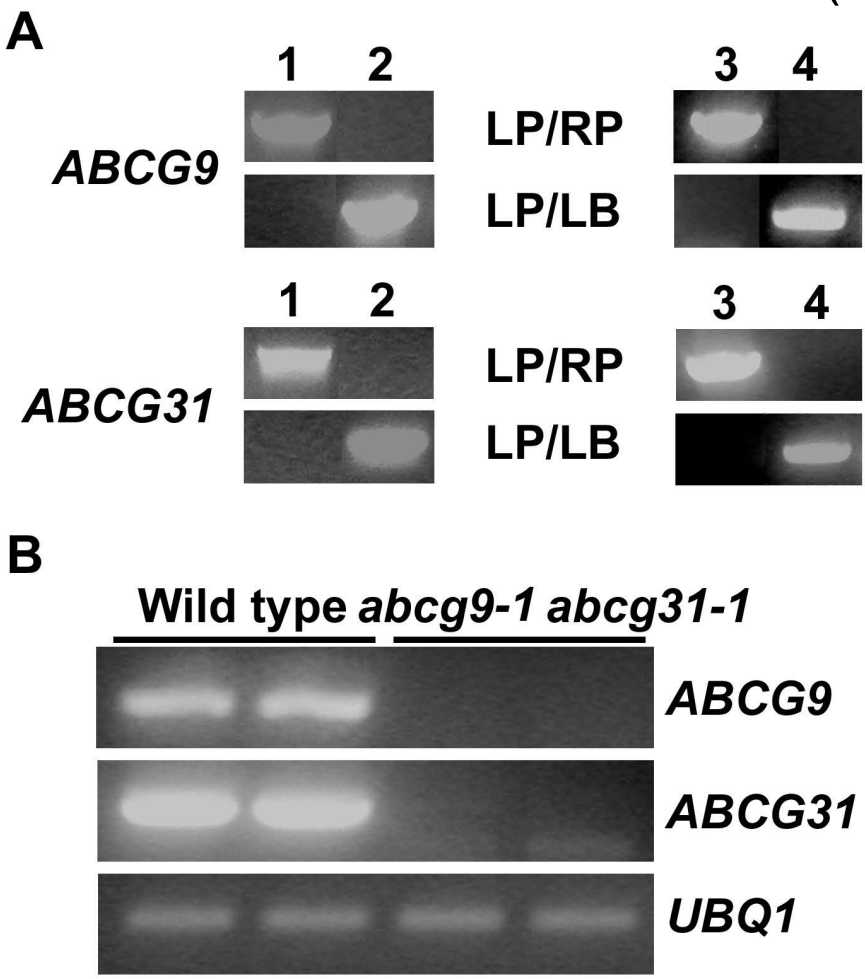

Supplemental Figure 4. Isolation of *abcg9 abcg31* double knockout mutant plants.

(A) Genomic DNA-PCR analysis of *ABCG9* and *ABCG31* in *abcg9-1 abcg31-1* and *abcg9-1 abcg31-2* plants. Total genomic DNA was extracted from the rosette leaves of wild-type (lanes 1 and 3), *abcg9-1 abcg31-1* (lane 2), and *abcg9-1 abcg31-2* (lane 4) plants. (B) RT-PCR analysis of *ABCG9* and *ABCG31* expression in the *abcg9-1 abcg31-1* mutant. Total RNA was extracted from the flowers of wild-type and *abcg9-1 abcg31-1* plants. *Ubiquitin* (*UBQ1*) was used as an internal control.

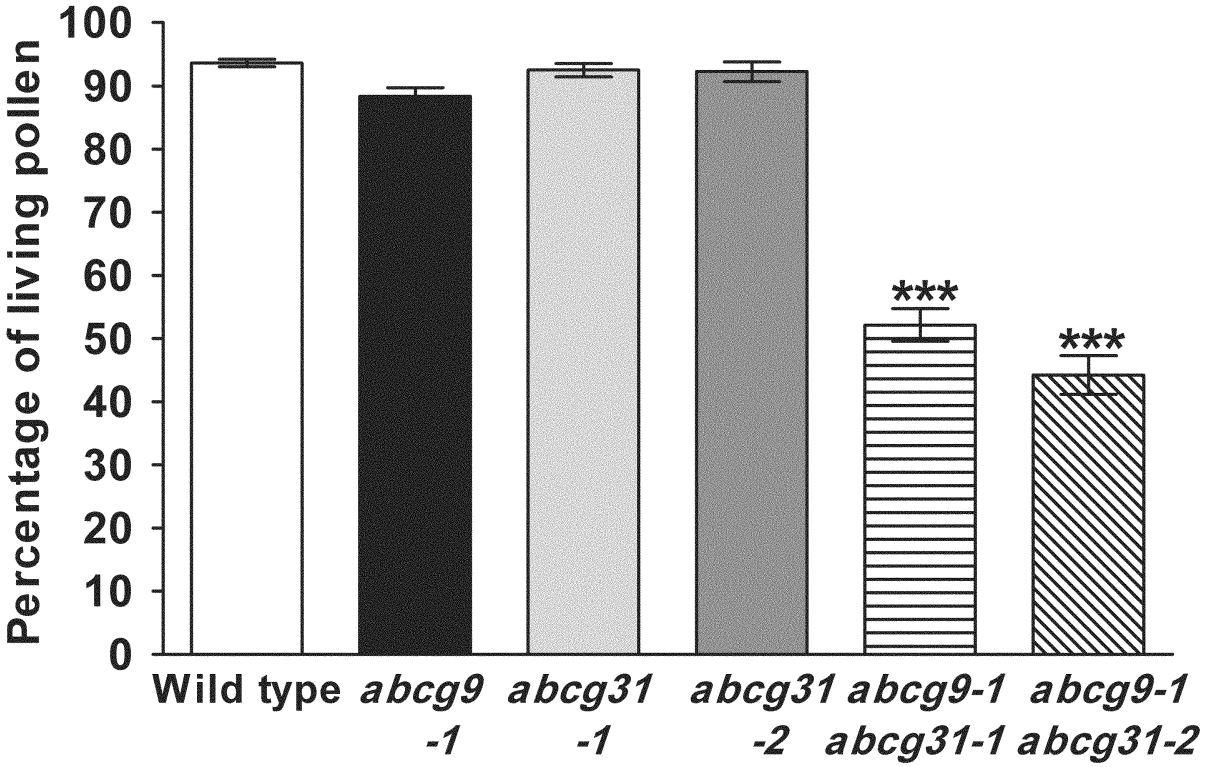

Supplemental Figure 5. Reduced pollen viability of *abcg9-1 abcg31-2* plants.

Pollen was collected from 4~5-week-old wild-type, *abcg9-1*, *abcg31-1*, *abcg31-2*, *abcg9-1 abcg31-1,* and *abcg9-1 abcg31-2* plants, and pollen viability was examined as described in Figure 2. The results from 29 (wild type, *abcg9-1,* and *abcg9-1 abcg31-1*), 16 (*abcg31-1*), 13 (*abcg31-2*), and 26 (*abcg9-1 abcg31-2*) flowers were combined. Data represent the means ± SE of two biological replicates. Statistical comparison was performed using one-way ANOVA followed by Tukey's multiple comparison test. ***: $P<0.001$ (compared to the wild type, *abcg9-1*, *abcg31-1*, and *abcg31-2*).

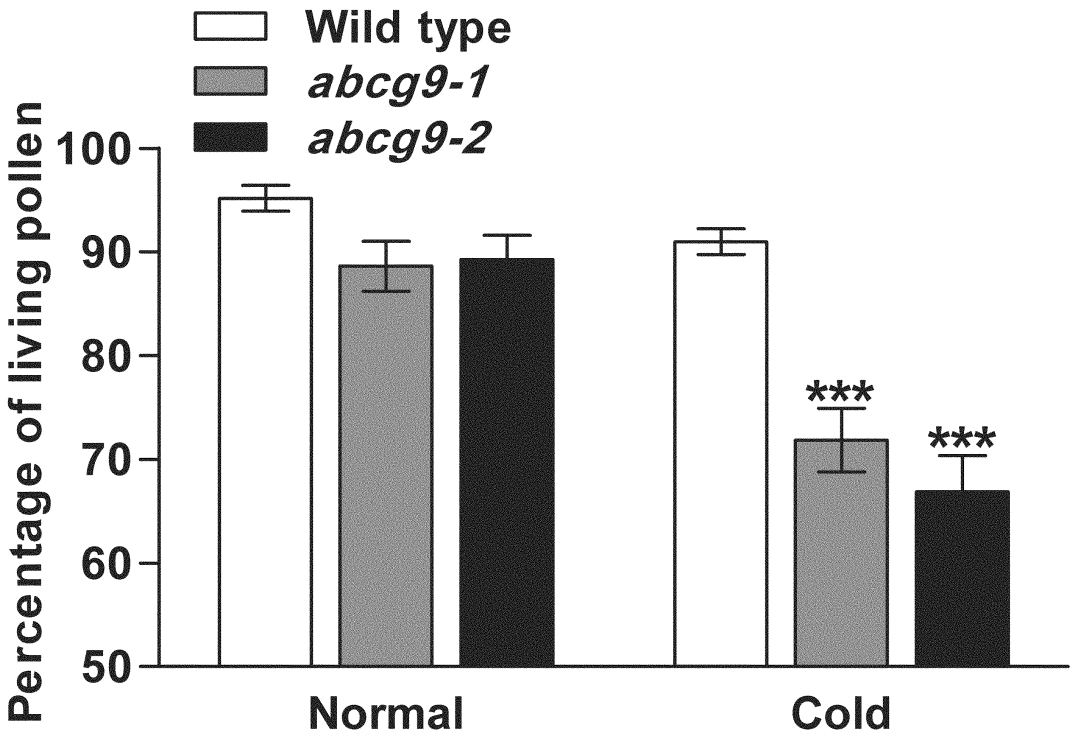

Supplemental Figure 6. Reduced pollen viability of *abcg9* plants after cold shock.

Pollen viability of wild-type and *abcg9* plants under normal growth conditions and after cold shock. For cold shock treatment, four-week-old plants were incubated at 4℃ for three days, and pollen viability was examined as described in Figure 2. The results from 13 and 18 flowers were combined, respectively. Data represent the means ± SE of two biological replicates. Statistical comparison was performed using one-way ANOVA followed by Tukey's multiple comparison test. ***: $P<0.001$ (compared to the wild type under normal or cold conditions, and *abcg9-1* and *abcg9-2* under normal conditions).

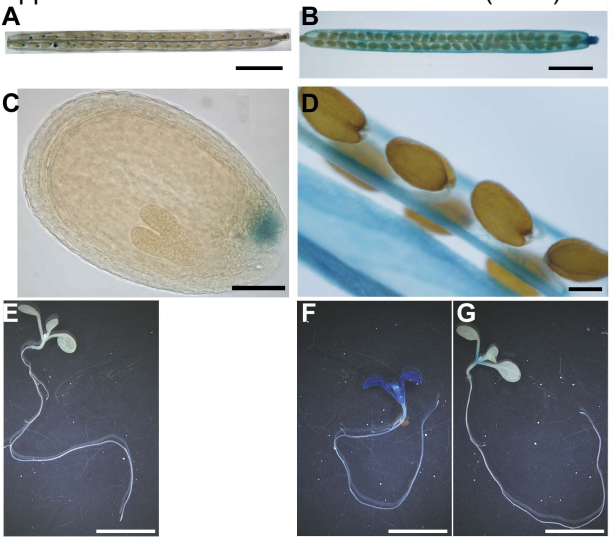

Supplemental Figure 7. The pattern of *ABCG9* and *ABCG31* expression in tissues other than flowers.

(A, B) GUS expression in a developing silique of a plant transformed with *ABCG9*$_{pro}$*:GUS* (A) or *ABCG31*$_{pro}$*:GUS* (B). Bars = 1 mm. (C) A developing seed from a *ABCG9*$_{pro}$*:GUS* plant displaying GUS signal in the chalaza. Bar = 100 μm. (D) No GUS expression was detected in the seeds of the *ABCG31pro:GUS* plant. Bar = 200 μm. (E) to (G) GUS expression in 9-day-old seedlings transformed with *ABCG9*$_{pro}$*:GUS* (E) or *ABCG31pro:GUS* (F, G). Bars = 0.5 mm. (E) No GUS expression was found in *ABCG9pro:GUS* seedlings. (F, G) GUS expression patterns in *ABCG31pro:GUS* seedlings. (F) Lines with higher expression exhibit signal mainly in the root vasculature and shoots. (G) Lines with lower expression exhibit signal only in the tips of the cotyledons and the basal parts of petioles.

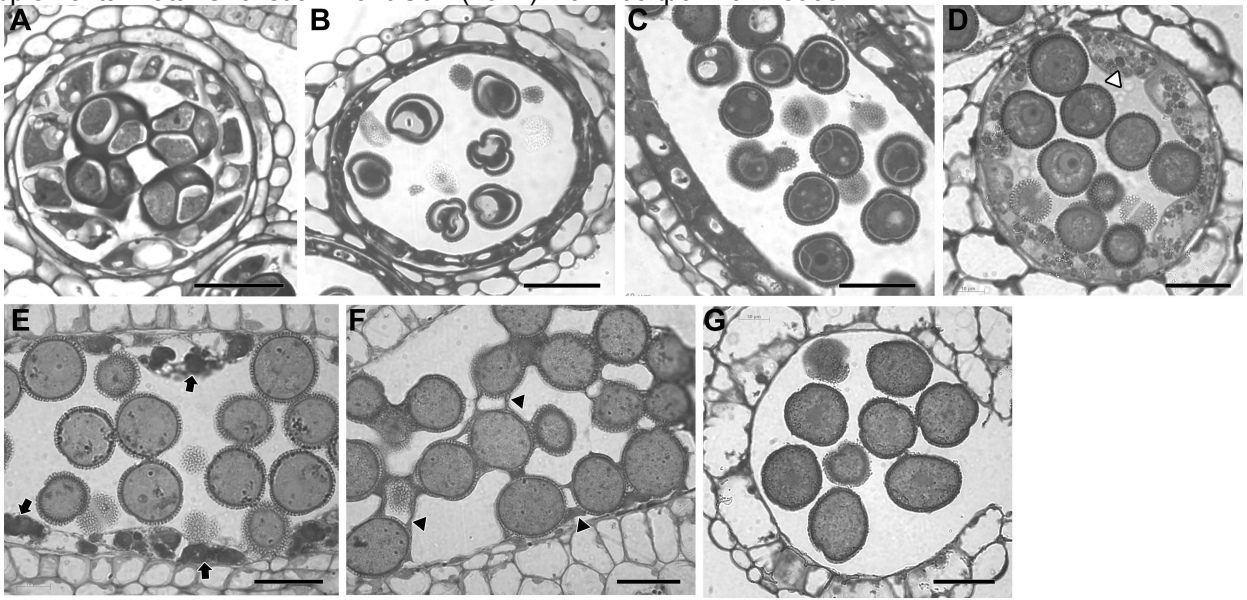

Supplemental Figure 8. Normal pollen development in *abcg9-1 abcg31-1* plants.

There was no visible defect in the pollen development of *abcg9-1 abcg31-1* plants. (A) Tetrad stage. (B) Vacuolate stage. (C) Mitosis I stage. (D) Bicellular stage. Lipidic compounds (arrowhead) accumulated in the tapetum. (E) Bi-/tri-cellular stage just prior to tapetal lysis. Tapetal cells are filled with an electron-dense substance, probably pollen coat materials (arrows). (F) Tricellular stage. Pollen coat materials released from the tapetum are deposited on the surface of pollen (arrowheads). (G) Mature stage. For pollen development in the wild type, see Figure 3 in Choi et al. (2010). Bars = 20 μm.

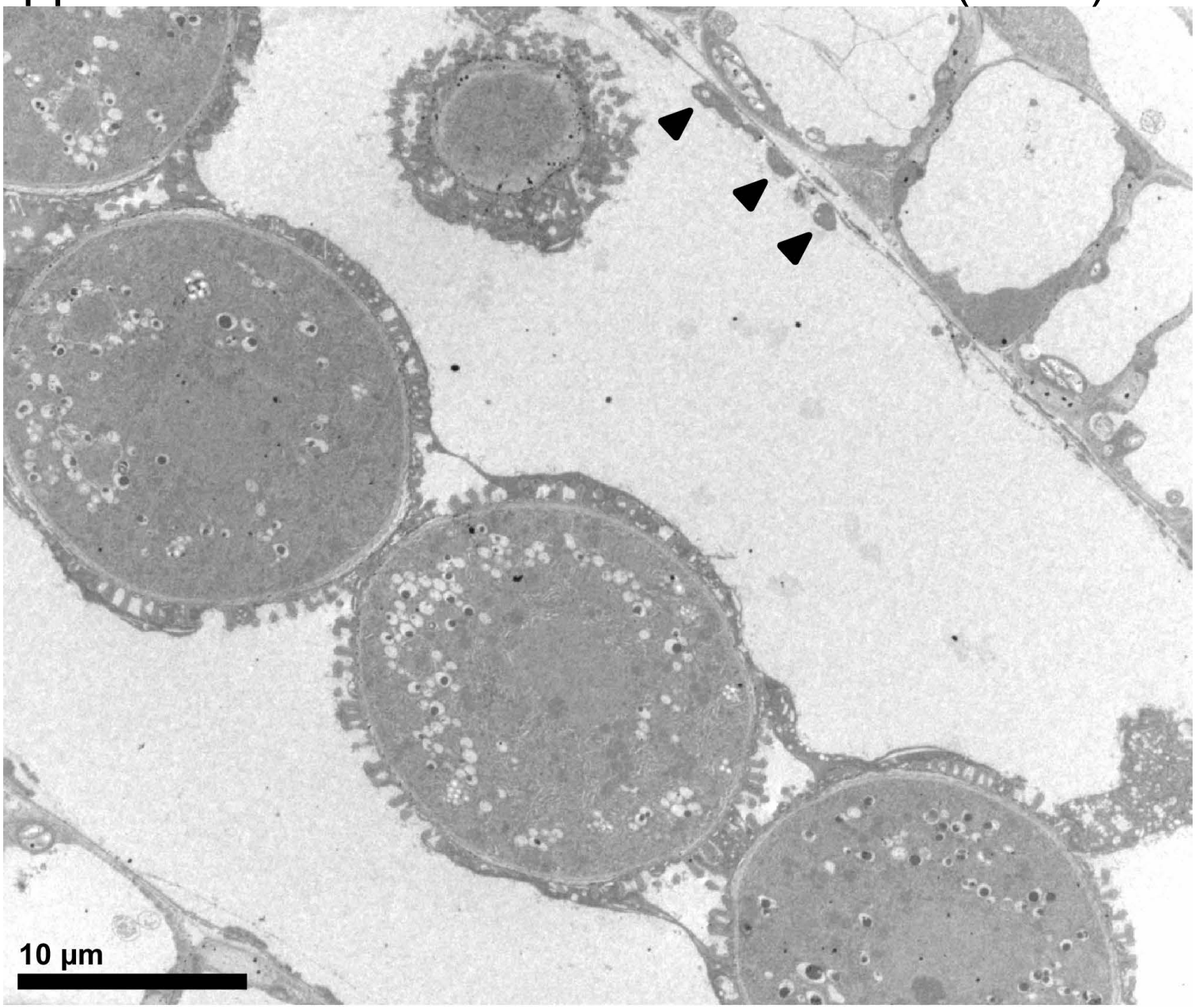

Supplemental Figure 9. Wild-type pollen grains at the beginning of pollen coat deposition. The tapetum is almost completely degraded (black arrowheads), and the pollen coat material released from the tapetum has not yet completely covered the surface of pollen grains. Bar = 10 µm.

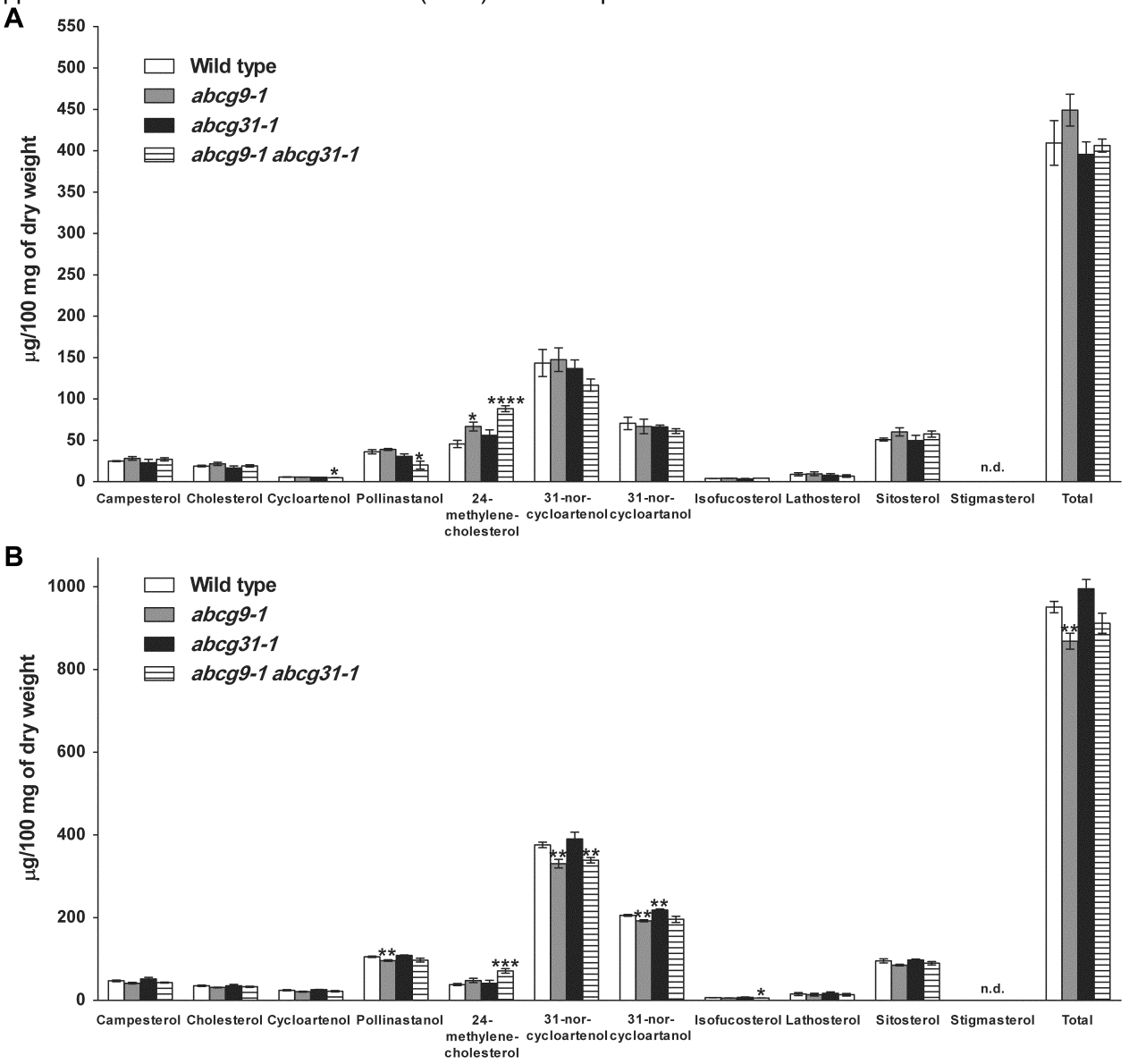

Supplemental Figure 10. Free sterol and steryl ester contents in wild-type, *abcg9-1*, *abcg31-1*, and *abcg9-1 abcg31-1* pollen.

Pollen was collected from 4-week-old wild-type, *abcg9-1*, *abcg31-1*, and *abcg9-1 abcg31-1* plants. Free sterol (A) and steryl ester (B) fractions were extracted, and separated according to sterol moiety using GC-MS. From about 50 mg of pollen sample, three independent lipid extractions and separations were executed. Data represent the means ± SE of two biological replicates (Student's *t*-test, *: $P<0.05$, **: $P<0.01$, ***: $P<0.001$, and ****: $P<0.0001$). n.d., not detected. Pollinastanol, 31-norcycloartnanol, and 31-norcycloartenol are tentative compounds, which were deduced by a comparison of mass fragmentation patterns with those reported in previous studies (Wu et al., 1999).

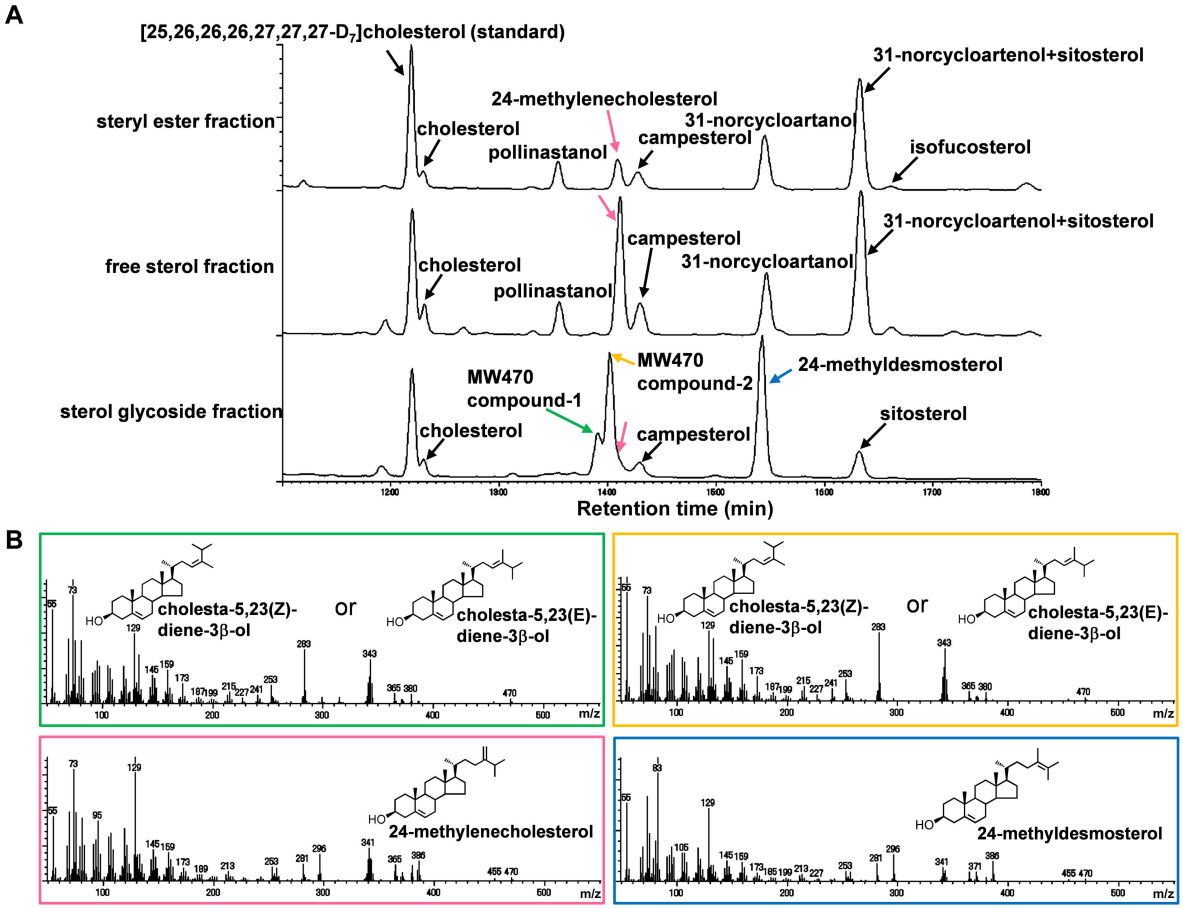

Supplemental Figure 11. Identification of MW470 sterol compounds.

(A) Gas chromatogram from the pollen sterol analysis (Figure 7). MW470 compound-1 (green) and -2 (orange) are unidentified compounds with similar molecular weight to 24-methylenecholesterol (magenta). (B) Mass fragmentograms of MW470 compounds (MW470 compound-1, green; MW470 compound-2, orange; 24-methylenecholesterol, magenta; 24-methyldesmosterol, blue). MW470 compound-1 and -2 displayed the same mass fragmentations, which are different from that of 24-methylenecholesterol. A comparison of the mass fragmentation patterns with those in previous studies suggests that these compounds are cholesta-5,23(Z)-diene-3β-ol or cholesta-5,23(E)-diene-3β-ol (Wretensjo and Karlberg, 2002).

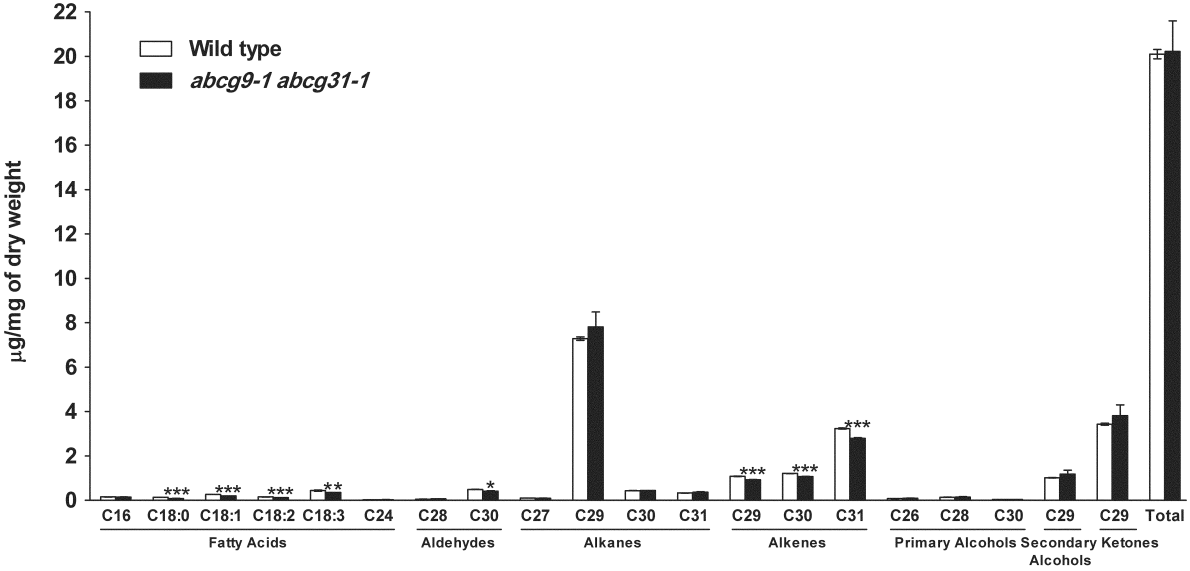

Supplemental Figure 12. Wax content in wild-type and *abcg9-1 abcg31-1* pollen.

Pollen was collected from 4-week-old wild-type and *abcg9-1 abcg31-1* plants. From about 50 mg of pollen sample, three independent lipid extractions and separations were executed. Data represent the means ± SE (Student's *t*-test, *: $P<0.05$, **: $P<0.01$, and ***: $P<0.001$).

Supplemental Table 1. Brassinosteroid content in wild-type and *abcg9-1 abcg31-1* pollen

Brassinosteroids	Wild type	*abcg9-1 abcg31-1*
6-Deoxocathasterone	3.20	2.75
6-Deoxoteasterone	n.d.	n.d.
3-Dehydro-6-deoxoteasterone	n.d.	n.d.
6-Deoxotyphasterol	n.d.	n.d.
6-Deoxocastasterone	6.60	6.40
Cathasterone	n.d.	n.d.
Teasterone	5.00	4.85
3-Dehydroteasterone	n.d.	n.d.
Typhasterol	18.0	17.5
Castasterone	44.0	41.0
Brassinolide	142	127
Total	219	199
Unit	pg/mg of dry weight	

n.d., not detected.

Supplemental Table 2. Primers used in this study

Isolation of knockout mutants		
abcg9-1 and *abcg9-2*	9LP	5'-ACCACTGCTCAAAGGATTGTGT-3'
	9RP	5'-CCTCAGCCAGATTTGGTCTTACCA-3'
abcg31-1	31LP1	5'-TGTCTCTGGAAACAGAACCT-3'
	31RP1	5'-TGACTGAAAGTGCAAATGCT-3'
abcg31-2	31LP2	5'-GAGTCTCTAGGATTCCGTCTC-3'
	31RP2	5'-CCCTTGCTAG AGAAGCCATCA-3'
T-DNA specific	LB1	5'-GCGTGGACCGCTTGCTGCAACT-3'
	LB2	5'-AACGTCCGCAATGTGTTATTAAGTTGTC-3'
	LB3	5'-ATAATAACGC TGCGGACATC TACATTTT-3'
TUB1	TUB1-F	5'-CTCACAGTCCCGGAGCTGACAC-3'
	TUB1-R	5'-GCTTCAGTGAACTCCATCTCGT-3'
UBQ1	UBQ1-F	5'-GCCAAGATCC AAGACAAAGA-3'
	UBQ1-R	5'-TTACGAGCAA GCATCATCAA-3'

Promoter-GUS expression assay		
ABCG9 promoter	Sal Ⅰ-ABCG9 proF	5'-GTCGAC-TCGAGAACCTACAAATAACAAGGT-3'
	Sma Ⅰ-ABCG9 proR	5'-CCCGGG-CCCCAACAATGATCGATCTATAAAG-3'
ABCG31 promoter	ABCG31 Pro-F	5'-CTCATCTGGTAGACTGCTAA-3'
	ABCG31 Pro-R	5'-CTCCATACCAACTCTACGAA-3'

Quantitative RT-PCR analysis		
ABCG9	9QRT-F	5'-ATGGATAATCAAGAGGTTTCTATG-3'
	9QRT-R	5'-TCATCTTGAGTCACGAAACCCG-3'
ABCG31	31QRT-F	5'-GGATCCTTCAGCTTTATGCAGA-3'
	31RP2	5'-CCCTTGCTAGAGAAGCCATCA-3'
PP2A	PP2A/A3-qRT-F	5'-TAACGTGGCCAAAATGATGC-3'
	PP2A/A3-qRT-R	5'- GTTCTCCACAACCGCTTGGT-3'

Complementation or overexpressing constructs		
ABCG9 complementation only	Sal Ⅰ-ABCG9 proF	5'-GTCGAC-TCGAGAACCTACAAATAACAAGGT-3'
	Sma Ⅰ-ABCG9 proR	5'-CCCGGG-CCCCAACAATGATCGATCTATAAAG-3'
ABCG9 complementation and overexpression	Xba Ⅰ-Smal Ⅰ-sGFP F	5'-TCTAGA-CCCGGG-ATGGTGAGCAAGGGCGAGGAGC-3'
	BamH Ⅰ-Ssp Ⅰ-5G-sGFP R	5'-GGATCC-AATATT-G GCC ACC TCC ACC TCC-CTTGTAC-3'
	Sac Ⅰ-Smal Ⅰ-ABCG9g F	5`-GAGCTC-CCCGGG-GG ATGGATAATCAAGAGGTTTCTAT-3`
	Pml Ⅰ-Xho Ⅰ-ABCG9g R	5'-CACGTG-CTCGAG-TATGCACCACAAATTCGTCAGCA-3'
ABCG31 overexpression	Nar Ⅰ-sGFP F	5'-GGCGCC-ATGGTGAGCAAGGGCGAGGAGC-3'
	BglⅡ-Spe Ⅰ-5G-sGFP R	5'- AGATCT-ACTAGT-GCC ACC TCC ACC TCC-CTTGTAC-3'
	Xba Ⅰ-ABCG31 F	5'-AA TCTAGA-ATGGCGGCGGCTTCGAATGG-3'
	BamH Ⅰ-ABCG31 R	5'-AA GGATCC TCCTCTTCTC TGGAAGTTGA-3'
	31LP1	5'-TGTCTCTGGAAACAGAACCT-3'
	attB3-ABCG31gR	5'-GGGGACAACTTTGTATAATAAAGTTGGTGAAGAGATCTTCGATGGGTCTCT-3'

Supplemental Table 3. Constructs

Use	Construct	Plasmid name	Insert or PCR product	Descrtiption	Primers	Template	Plasmid backbone	Cloning method
Promoter-GUS expression	ABCG9pro:GUS	Teasy-ABCG9pro	ABCG9 promoter	Upstream sequence	SalⅠ-ABCG9 proF SmaⅠ-ABCG9 proR	Arabidopsis genomic DNA	pGEM-T Easy Vector (Promega)	TA cloning
		pBIABCG9pro-GUS	ABCG9 promoter	-	-	Teasy-ABCG9pro	pBI101.2	SalI/SmaI
	ABGC31pro:GUS	pCR-topo-ABCG31pro	ABCG31 promoter	upstream sequence ~ part of the second exon	ABCG31 Pro-F ABCG31 Pro-R	Arabidopsis genomic DNA	pCR8-GW-TOPO (Invitrogen)	Topo-isomerase
		pMDCABCG31pro-GUS	ABCG31 promoter	-	-	pCR-topo-ABCG31pro	pMDC163 (Curtis and Grossniklaus, 2003)	Gateway LR
ABCG9 overexpression	35Spro:sGFP:ABCG9	Teasy-ABCG9 gDNA	ABCG9 genomic DNA	ORF+3'-untranslated region	SacⅠ-SmaⅠ-ABCG9g F PmlⅠ-XhoⅠ-ABCG9g R	Arabidopsis genomic DNA	pGEM-T Easy vector	TA cloning
		Teasy-sGFP	sGFP (green fluorescent protein)	sGFP with X 5 linker sequence	XbaⅠ-SmaⅠ-sGFP F BamHⅠ-SspⅠ-5G-sGFP R	p326 sGFP-3G (pUC vector based, kindly provided by professor Inhwan Hwang, POSTECH, Korea)	pGEM-T Easy vector	TA cloning
		pPZP221-35S-sGFP-ABCG9g-nosT	ABCG9 genomic DNA sGFP	-	-	Teasy-ABCG9 gDNA Teasy-sGFP	pPZP221-35S-nosT (Hajdukiewicz et al., 1994)	appropriate restriction enzymes
ABCG9 complementation	ABCG9pro:sGFP:ABCG9	pPZP221-ABCG9pro	ABCG9 promoter	-	-	Teasy-ABCG9pro	pPZP221	SalI/SmaI
		pPZP221-ABCG9pro-sGFP-ABCG9g-nosT	ABCG9 promoter	-	-	pPZP221-ABCG9pro	pPZP221-35S-sGFP-ABCG9g-nosT	appropriate restriction enzymes
ABCG31 overexpression	35Spro:sGFP:ABCG31	pCR-topo-ABCG31CDS	ABCG31CDS	Coding sequence	XbaⅠ-ABCG31 F attB3-ABCG31gR	Arabidopsis cDNA	pCR8-GW-TOPO	Topo-isomerase
		pCR-topo-ABCG31CDS partUTR	ABCG31CDS part	Part of coding sequence containing the last inrton+3'-untranslated region	31 LP1 attB3-ABCG31gR	Arabidopsis genomic DNA	pCR8-GW-TOPO	Topo-isomerase
		pCR-topo-ABCG31CDSUTR	ABCG31CDS part	Coding sequence containing the last inrton+3'-untranslated region	-	pCR-topo-ABCG31CDS partUTR	pCR-topo-ABCG31CDS	appropriate restriction enzymes
		pCR-topo-sGFP	sGFP	sGFP with X 5 linker sequence	NarⅠ-sGFP F BglⅡ-SpeⅠ-5G-sGFP R	p326 sGFP-3G	pCR8-GW-TOPO	Topo-isomerase
		pCR-topo-sGFP-ABCG31CDSUTR	sGFP	-	-	pCR-topo-sGFP	pCR-topo-ABCG31CDSUTR	appropriate restriction enzymes
		pMDC32-sGFP-ABCG31CDSUTR	sGFP-ABCG31 CDSUTR	-	-	pCR-topo-sGFP-ABCG31CDSUTR	pMDC32 (Curtis and Grossniklaus, 2003)	Gateway LR

Supplemental Methods

Comparison of the steryl glycoside content on the surface of individual pollen and leaf cells

Steryl glycosides are known to be mainly localized to the plasma membrane; thus, if steryl glycosides are also present as normal components of the pollen coat, pollen should have a much higher steryl glycoside content per unit surface area of the cell than other types of cells, such as leaf cells. To evaluate this possibility, we sought to compare the steryl glycoside content per unit surface area of pollen versus that of leaf cells. Whereas the steryl glycoside content per dry weight was known, the number of cells per unit weight was not. We thus estimated steryl glycoside content based on the volume of the cells.

First, we converted the steryl glycoside content per unit dry weight into a value per unit fresh weight, because we reasoned that the cell volume is better correlated with fresh weight than with dry weight, which is obtained from tissues that have been deformed during the drying process. Water accounts for 90% of the total volume of a leaf cell and for 50% of that of a pollen, which is already dehydrated (Barnaba, 1985). Since the steryl glycoside content was 25 and 70 μg/100 mg of the dry weight of leaves and pollen, respectively (Figure 8, DeBolt et al., 2009), the corresponding values in fresh weight were 2.5 and 35 μg/100 mg of fresh weight, respectively.

Next, we calculated the total surface area of leaf and pollen cells occupying a given space. Assuming that a cell is spherical, we used the equation for the surface area of a sphere, $S = 4\pi r^2$, to obtain the cell surface area. The total surface area of the cells in a space can be obtained by multiplying the surface area of each cell by the number of cells (N) in the space. Fewer large cells occupy a given space than small

cells. Thus, the number of cells in a specific volume is N=1/(V of each cell). The V of each cell was estimated to be the V of a sphere, $^4/_3\pi r^3$. Thus, the total surface area is $S_{total} = S_{single\ cell} \times N = 4\pi r^2 \times 1/(^4/_3\ \pi r^3) = 3/r$. The average radius, r, of a leaf mesophyll cell and a pollen grain is 25 and 10 μm, respectively. Finally, to calculate the steryl glycoside content per unit surface area, the content was divided by the surface area. Thus, the ratio of steryl glycoside content in leaf cells to that in pollen is $2.5/(^3/_{25}):35/(^3/_{10})$, which is equal to 1:5.6. Therefore, a pollen grain is estimated to contain 5.6 times more steryl glycosides at the plasma membrane and on the surface than does a leaf cell.

Supplemental References

Barnaba, B. (1985). Effect of water loss on germination ability of maize (*Zea mays L.*) pollen. Ann. Bot. **55:** 201-204.

Curtis, M.D., and Grossniklaus, U. (2003). A Gateway cloning vector set for high-throughput functional analysis of genes in planta. Plant Physiol. **133:** 462-469.

DeBolt, S., Scheible, W.R., Schrick, K., Auer, M., Beisson, F., Bischoff, V., Bouvier-Nave, P., Carroll, A., Hematy, K., Li, Y., Milne, J., Nair, M., Schaller, H., Zemla, M., and Somerville, C. (2009). Mutations in UDP-Glucose:sterol glucosyltransferase in *Arabidopsis* cause transparent testa phenotype and suberization defect in seeds. Plant Physiol. **151:** 78-87.

Hajdukiewicz, P., Svab, Z., and Maliga, P. (1994). The small, versatile pPZP family of *Agrobacterium* binary vectors for plant transformation. Plant Mol. Biol. **25:** 989-994.